



# The subthreshold micropulse laser treatment of the retina restores the oxidant/antioxidant balance and counteracts programmed forms of cell death in the mice eyes

Stefano De Cillà,<sup>1</sup>  Diego Vezzola,<sup>2</sup> Serena Farruggio,<sup>2,3</sup> Stela Vujosevic,<sup>1</sup> Nausicaa Clemente,<sup>4</sup> Giulia Raina,<sup>2,3</sup> David Mary,<sup>2,3</sup> Giamberto Casini,<sup>5</sup> Luca Rossetti,<sup>6</sup> Laura Avagliano,<sup>7</sup> Carla Martinelli,<sup>7</sup> Gaetano Bulfamante<sup>7</sup> and Elena Grossini<sup>2,3</sup> 

<sup>1</sup>Ophthalmology Unit, Department of Health Sciences, Azienda Ospedaliera Universitaria Maggiore della Carità, University of East Piedmont, Novara, Italy

<sup>2</sup>Lab. Physiology/Experimental Surgery, Department of Translational Medicine, University of East Piedmont, Novara, Italy

<sup>3</sup>AGING Project, Department of Translational Medicine, University of Eastern Piedmont, Novara, Italy

<sup>4</sup>Lab. Immunology, IRCAD, Department of Health Sciences, University East Piedmont, Novara, Italy

<sup>5</sup>Department of Surgical, Medical, Molecular and Critical Area Pathology, University of Pisa, Pisa, Italy

<sup>6</sup>Eye Clinic, San Paolo Hospital, University of Milan, Milan, Italy

<sup>7</sup>Pathological Anatomy, Department of Health Sciences, San Paolo Hospital, University of Milan, Milan, Italy

## ABSTRACT.

**Purpose:** Subthreshold micropulse laser (SMPL) has been increasingly used for the treatment of different retinal and choroidal macular disorders. However, the exact mechanisms of action have not yet been clearly defined. Therefore, we aimed to examine the role of SMPL treatment in the modulation of oxidant/antioxidant systems, apoptosis and autophagy in the mice eyes.

**Methods:** A specific laser contact lens for retina was positioned on the cornea of 40 mice (20 young and 20 old) in order to focus the laser on the eye fundus for SMPL treatment. Within 6 months, 20 animals received one treatment only, whereas the others were treated three times. Eye specimens underwent histological analysis and were used for thiobarbituric acid reactive substances (TBARS) and glutathione (GSH) quantification, as well as for the superoxide dismutase 1 (SOD1) and the selenoprotein thioredoxin reductase 1 (TrxR1) expression evaluation. Western blot was performed for nitric oxide synthase (NOS) subtypes detection and to examine changes in apoptotic/autophagy proteins expression.

**Results:** SMPL treatment reduced TBARS and increased GSH and SOD1 in the mice eyes. It also reduced cytochrome *c*, caspase 3 expression and activity and cleaved caspase 9, and increased Beclin 1, p62 and LC3 $\beta$ . The effects were more relevant in the elderly animals.

**Conclusion:** Our results showed that SMPL therapy restored the oxidant/antioxidant balance within retinal layers and modulated programmed forms of cell death. Further studies may confirm these data and could evaluate their relevance in clinical practice.

**Key words:** apoptosis – autophagy – laser therapy – nitric oxide – oxidative stress

Acta Ophthalmol.

© 2018 Acta Ophthalmologica Scandinavica Foundation. Published by John Wiley & Sons Ltd

doi: 10.1111/aos.13995

## Introduction

Subthreshold micropulse laser (SMPL) treatment is currently used in different retinal diseases, including diabetic macular oedema, central serous chorioretinopathy and macular oedema secondary to retinal vein branch occlusion (BRVO) (Vujosevic et al. 2010, 2013, 2015; Maruko et al. 2017).

The molecular mechanisms involved in these conditions include increased oxidative stress, which increases cellular permeability and tight junction disruption (Amoaku et al. 2015). Also, apoptosis and endothelial and inducible nitric oxide synthase (NOS)-dependent nitric oxide (NO) release could be involved as pathogenetic factors (Zhang et al. 2014).

Thus, although the exact mechanisms of reducing oedema by laser therapy have not so far been clearly examined, a plausible role would be played by the modulation of retinal oxygenation/metabolism and oxidative stress (Vujosevic et al. 2013; Amoaku et al. 2015).

However, the use of the suprathreshold laser photocoagulation is associated with many side-effects, including

chorioretinal atrophy, choroidal neovascularization, formation of fibrotic scars and reduced retinal sensitivity. Those complications can be limited by changing laser parameters, such as power and wavelength, spot size of retinal irradiance, pulse duration and the use of micropulse technique (Mainster 1999; Ferrara et al. 2003; Kiire et al. 2011).

Hence, the laser treatment technique has turned over the years into a more advanced, effective and safe therapy for retinal disorders. The new technique takes advantage of subthreshold, micropulses of controlled laser radiations that are selectively absorbed by the retinal pigment epithelium (RPE) and therefore can elicit therapeutic effects with minimal or no retinal damage (Ohkoshi & Yamaguchi 2010; Luttrull et al. 2012; Li et al. 2015). As mentioned above, however, available data regarding the cellular mechanisms are scarce.

We therefore planned to examine the histological and molecular effects of micropulse laser in young and old mice eyes. Particular attention was paid to the balance between oxidant/antioxidant system, NOS subtypes and markers of apoptosis and autophagy expression/activation.

## Materials and Methods

The experiments were performed in 40 male C57BL/6 mice. Twenty mice were 3 months old (young) (Lutty 2017) at the beginning of the treatment, whereas the others were 12 months old (old) (Dutta & Sengupta 2016). All mice were housed in a room at a constant temperature of 25°C on a 12-/12-hr light/dark cycle with food and water available *ad libitum*. All experiments were conducted in accordance with local ethical standards, approved by national guidelines (legislative decree (DLGS), January 27, 1992, license 116) and in accordance with ARRIVE guidelines and with ‘Guide for the Care and Use of Laboratory Animals’ (National Institutes of Health publication 8023, 1978 revision).

For laser treatment, a specific laser contact lens for retina (Ocular Fundus 5.4 LASER lens; Ocular Instruments New Tech SpA, Vimodrone, Milan, Italy) was positioned on the cornea in order to focus the laser on the eye fundus. Mice were previously anaesthetized with

intramuscular ketamine (50 mg/kg; Intervet, Segrate, Milan, Italy), xylazine (5 mg/kg; Bayer, Varese, Italy) and acepromazine (0.5 mg/kg; Bayer) administered 15 min before the procedure. One drop of 1% tropicamide (Novartis Farma, Origgio, Varese, Italy) and 2.5% phenylephrine hydrochloride (Novartis Farma) were topically applied 30 min prior to laser micropulse procedure to achieve pupillary dilation. A micropulse infrared laser 810 nm (Ocu-light SLx; Iridex, Corp, Mountain View, CA, USA) positioned on a specific slit lamp was used. The laser parameters established through a ‘burn test’ were as follows: spot size, 500 µm; pulse time, 75 ms and 50 mWatt until barely visible retinal whitening in a continuous mode. The laser power was duplicated in the micropulse mode with application of confluent spots. In all eyes, a visible burn was obtained with 50 mWatt with continuous wave mode; therefore, 100 mWatt power was used in micropulse mode at 5% in order not to have clinically visible treatment. Laser treatment was performed on all visible retina from optic disc till periphery, trying to be more confluent as possible. At least an area of 2.0 mm radius from the optic disc (four laser spot diameters) was treated (Fig. 1).

As shown in Fig. 2, mice were divided into two groups: only one-treatment group ( $n = 20$ ) and three-treatment group ( $n = 20$ ). In the only one-treatment group, the laser treatment was applied to the left eye at month 1 (T1). In the three-treatment group, the laser treatment was applied to the left eye once every 3 months for

6 months from month 1 (T1) to month 6 (T3). The time interval of 3 months for retreatment was chosen as per usual clinical practice and based on data from randomized clinical trial (Vujosevic et al. 2015). Each treatment lasted about 5 min. The nontreated eye of each mouse was used as a control.

At 1 month after the last treatment, all animals were sacrificed through cervical dislocation and eyes were gently removed and either placed in phosphate-buffered saline (PBS; Sigma, Milan, Italy) on ice for molecular analysis or fixed in 2.5% glutaraldehyde in phosphate buffer 0.13 M (Sigma) for histology.

### Tissue preparation for molecular analysis

Using a dissecting microscope, seven eyes for each experimental group were incised at the posterior margin of the limbus and the cornea, and the iris and lens were removed. Thereafter, the retinas were lifted away from the eyecup by forceps and sectioned for further analysis (Wei et al. 2016). In particular, for TBARS and Western blot analysis, retinas were lysed in a buffer (1 M Tris base, 1 M NaCl, 0.5 M EDTA, 10% nonyl phenoxypolyethoxyethanol and 10% Triton X-100; Sigma) containing 1:100 protease inhibitors, 1:200 sodium orthovanadate and 1:1000 phenylmethylsulfonyl fluoride (Sigma) and homogenized on ice by using homogenizer (Microtec Co., Ltd., Chiba, Japan). The lysates were centrifuged at 14 000 *g* for 20 min at 4°C, and the supernatant was used for the analysis.

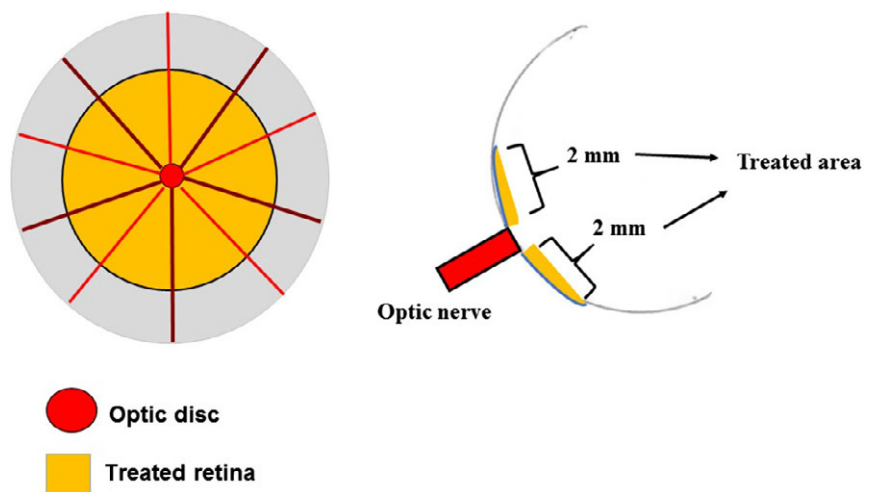


Fig. 1. Schematic representation of the eye fundus treated by laser.

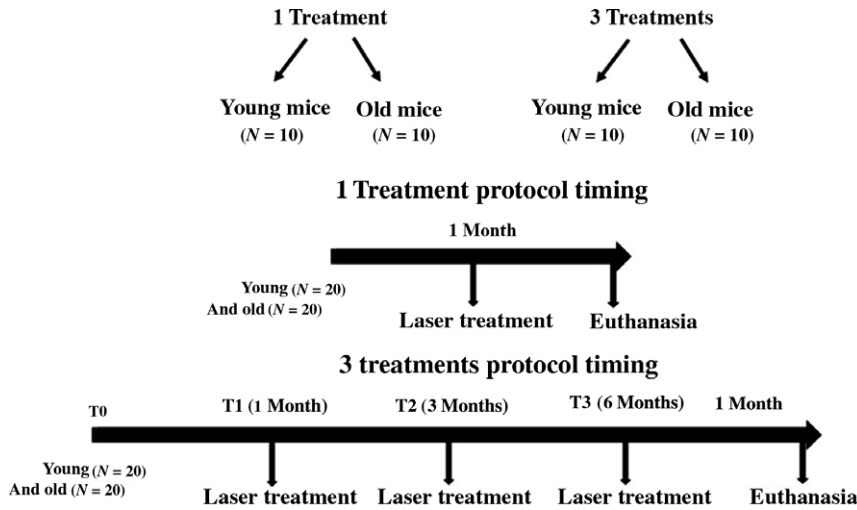


Fig. 2. Schematic representation of the experimental protocol.

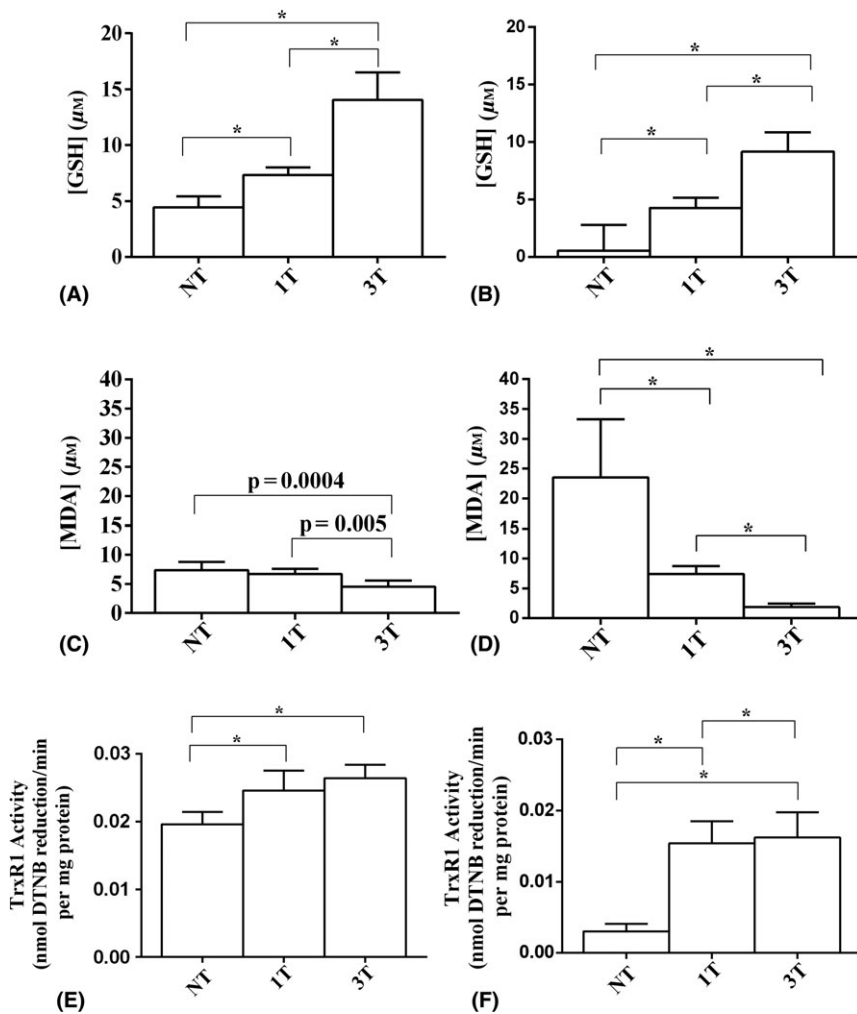


Fig. 3. Effects of SMPL on glutathione (GSH), malonyldialdehyde (MDA) and thioredoxin reductase 1 (TrxR1) retinal content in young (A, C, E) and old (B, D, F) mice. The results are shown as the mean  $\pm$  SD of four or seven different experiments. NT: nontreated eye; IT: one laser treatment; 3T: three laser treatments. Square brackets indicate significance between groups. \* $p < 0.0001$ .

For glutathione (GSH) quantification, retinas were washed many times with PBS (Sigma) to remove any red blood cells. Thereafter, retinas were homogenized in 5 ml of cold buffer (MES buffer; Sigma) per gram tissue. The homogenized tissues were centrifuged at 10 000  $g$  for 15 min at 4°C, and supernatant was used for the analysis.

**Optical microscopy**

Histological analysis was performed in the same area treated with laser by the same researcher blinded to the experimental protocol on three eyes from each experimental group. The posterior segment (that includes choriocapillaris, Bruch’s membrane, RPE and neuroretina) of the eye was fixed in osmium tetroxide in 0.1 M cacodylate buffer (Sigma) for 1 h, subjected to dehydration, then embedded in epoxy resin and sectioned into 1-μm semithin sections and analysed by optical microscopy.

**Thiobarbituric acid reactive substances (TBARS) assay**

For TBARS quantification, the manufacturer’s instructions were followed (Cayman Chemical, Ann Arbor, MI, USA), as previously performed (Grossini et al. 2014; Surico et al. 2015).

Briefly, 100 μl of each sample was complemented with an equal volume of a sodium dodecyl sulphate solution, supplemented with 4 ml of a colour reagent and vortexed. The samples were then incubated at 95°C for 60 min, placed in an iced bath to stop the reaction for 10 min and centrifuged (10 min at 1600  $g$  at 4°C). Thereafter, 150 μl of each sample was loaded in a 96-well plate and the absorbance was measured with a spectrometer (BS1000 Spectra Count, San Jose, CA, USA) at 530 nm. The results were presented as micromolar concentrations of malondialdehyde (MDA).

**GSH assay**

GSH measurements were performed with a specific kit (Cayman Chemical), as previously performed (Grossini et al. 2014; Surico et al. 2015; De Cilla et al. 2017).

The supernatant was treated with an equal volume of metaphosphoric acid



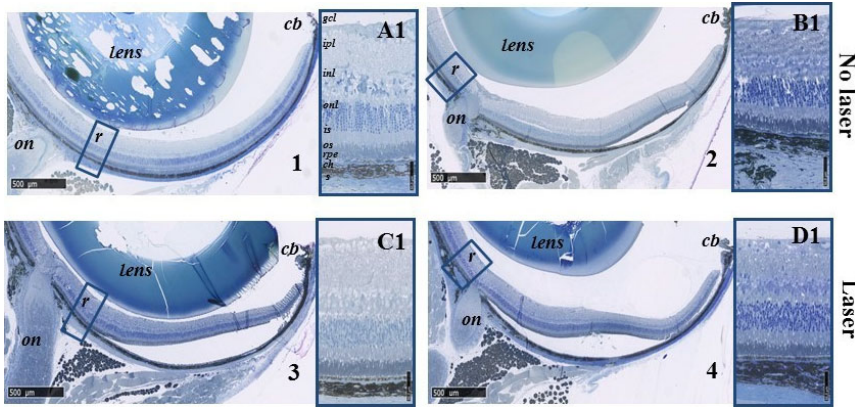


**Fig. 4.** Histological analysis of mice eyes. An example taken from 3 different eyes for each experimental group is shown. In 1 and 2, the histological analysis of retinas from the nontreated eye of each treated animal is shown. In 3 and 4, the histological analysis of retinas from the three-treatment animal group is shown. A1-D1: all retinal layers. Cb = ciliary body; On = optic nerve; GCL = ganglionic cell layer, IPL = inner plexiform layer, INL = inner nuclear layer, ONL = outer nuclear layer, IS = photoreceptor inner segments, OS = photoreceptor outer segment, RPE = retinal pigmented epithelium, Ch = choroids, S = sclera.

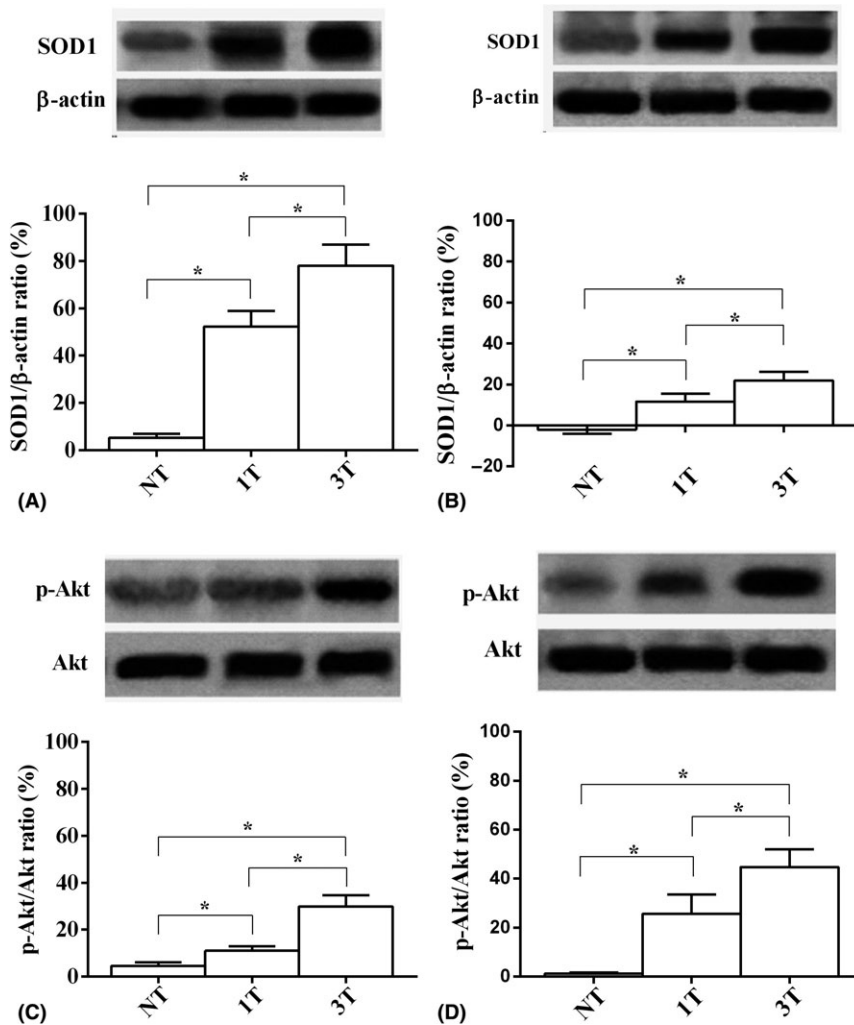


**Fig. 5.** Effects of SMPL on retinal superoxide dismutase 1 (SOD1) and Akt activation in young (A, C) and old (B, D) mice. In (A, B) expression of SOD1; in (C, D) activation of Akt. Densitometric analysis and an example of Western Blot, taken from seven different experiments, are shown. Abbreviations are as in previous Figures. The results are the means  $\pm$  SD of seven different experiments. Square brackets indicate significance between groups. \* $p < 0.0001$ .

(final concentration 5%; Sigma-Aldrich Corp., St. Louis, MO, USA) for 5 min and centrifuged at 2000 *g* for at least two min. The supernatant was collected and supplemented with 50  $\mu$ l per ml of 4 M solution of triethanolamine (Sigma). Fifty  $\mu$ l of the samples was transferred to a 96-well plate where GSH was detected following the manufacturer's instructions through a spectrometer (BS1000 Spectra Count) at excitation/emission wavelengths of 405–414 nm. GSH was expressed as nanomoles in samples with 1.5 mg of protein/ml.

**Thioredoxin reductase colorimetric assay**

Thioredoxin reductase 1 (TrxR1) activity was measured with a specific kit (Cayman Chemical), by monitoring the nicotinamide adenine dinucleotide phosphate (NADPH)-dependent reduction of DTNB (5,5'-dithiobis(2-nitrobenzoic) acid) in the presence or absence of aurothiomalate (ATM), a specific TrxR1 inhibitor. Briefly, 20  $\mu$ l of each sample was transferred to a 96-well plate where TrxR1 was detected. The reactions were initiated by adding 0.24 mM NADPH and 3 mM DTNB and the rate of increase in absorbance was measured at 405 nm, following the manufacturer's instructions, through a spectrometer (BS1000 Spectra Count). The amount of NADPH-dependent activity that was inhibited by ATM is attributed to TrxR1. TrxR1 activity was expressed as nmol DTNB reduction/min per mg protein.

**Caspase 3 activity assay**

The effect of micropulse laser treatment on caspase 3 activity was determined by using a commercially available Mouse Casp 3 (Caspase 3) ELISA kit (Fine Test, Wuhan, Hubei, China), following the manufacturer's instructions. Briefly, 100  $\mu$ l of each sample, diluted 1:10 in wash buffer (tissue homogenate concentration was 10–100 ng/ml), was added into test sample wells and incubated at 37°C for 90 min. Samples were aspirated and washed two times with wash buffer and incubated with 100  $\mu$ l of biotin-labelled antibody working solution for 60 min at 37°C. After removal of the antibody solution, the wells were washed again and incubated with 100  $\mu$ l of HRP-streptavidin conjugate (SABC)

working solution, for 30 min at 37°C. After the aspiration of the SABC working solution, blue colour was developed by adding 90 µl of TMB substrate into each well. The chromogen solution was incubated for 15–30 min in the dark. The reaction was stopped by adding 50 µl of stop solution, and the yellow colour developed was read using a microplate reader at 450 nm.

**Nitrate and nitrite colorimetric assay**

For total nitrate and nitrite quantification, the manufacturer’s instructions were followed (Cayman Chemical). Briefly, tissue samples were homogenized and centrifuged at 10 000 g for 20 min. The supernatant was ultracentrifuged at 10 000 g for 30 min and then ultrafiltered by using 30 kDa molecular weight cut-off filter. For total nitrate and nitrite measurement, 40 µl of each filtrate was diluted in 40 µl assay buffer, and 80 µl of each diluted sample was transferred to a 96-well plate. Ten µl of the enzyme cofactor mixture and 10 µl of the nitrate reductase mixture were added in each well (standards and unknowns). The plate was covered and incubated at room temperature for 3 h. Finally, 50 µl of Griess reagent R1, followed by the addition of 50 µl of Griess reagent R2, was added in each well. After 10 min, the total nitrate and nitrite production was measured through a spectrometer (BS1000 Spectra Count), reading the absorbance at 540 nm. The results were presented as micromolar concentrations of nitrate and nitrite.

**Western blotting**

Protein concentrations were determined by using the bicinchoninic acid (Pierce, Rockford, IL, USA) assay. Cell lysates (30 µg protein each sample) dissolved in Laemmli buffer 5×, boiled for 5 min, were resolved in 15% sodium dodecyl sulphate (Sigma) polyacrylamide gel electrophoresis (Bio-Rad Laboratories, Hercules, CA, USA), and after electrophoresis, transferred to polyvinylidene fluoride membranes (Bio-Rad Laboratories) which were incubated overnight at 4°C with specific primary antibodies: anti-phospho-Akt (1:1000; Ser473; Cell Signalling Technologies, Danvers, MA

USA), anti-Akt (1:1000; Cell Signalling Technologies), anti-phospho-endothelial NOS (eNOS; 1:1000; Ser1177; Cell Signalling Technologies), anti-eNOS (1:1000; Cell Signalling Technologies), anti-inducible NOS (iNOS; 1:500; Santa Cruz Biotechnology, Inc., CA, USA), anti-cytochrome c (1:500; Sigma), anti-cleaved caspase 9 (1:1000; Cell Signalling Technologies), anti-caspase 3 (1:500; Santa Cruz Biotechnology), anti-Bcl-1 (Bcl1; 1:500; Santa Cruz Biotechnology), anti-MAP LC3 α/β (1:500; H-47; Santa Cruz Biotechnology), anti-superoxide dismutase 1 (SOD-1; 1:500; Santa Cruz Biotechnology) and anti-p62 (1:500; CABRU, Arcore, Milan, Italy). The membranes were washed and then incubated with horseradish peroxidase-coupled goat anti-rabbit IgG (Sigma), peroxidase-coupled rabbit anti-goat IgG and horseradish peroxidase-coupled goat anti-mouse IgG (Sigma) for 45 min, and were

developed through a nonradioactive method using Western Lightning Chemiluminescence (PerkinElmer Life and Analytical Sciences, Waltham, MA, USA). Phosphorylated protein expression was calculated as a ratio towards specific total protein expression or β-actin (1:5000; Sigma) detection.

**Statistics**

All data were recorded using the Institution’s database. Statistical analysis was performed using STATVIEW version 5.0.1 for Microsoft Windows (SAS Institute Inc., Cary NC, USA). Data were checked for normality before statistical analysis. One-way ANOVA followed by Bonferroni post hoc tests were used to examine changes in different groups of animals. Data are expressed as means ± standard deviation (SD). A value of p < 0.05 was considered statistically significant.

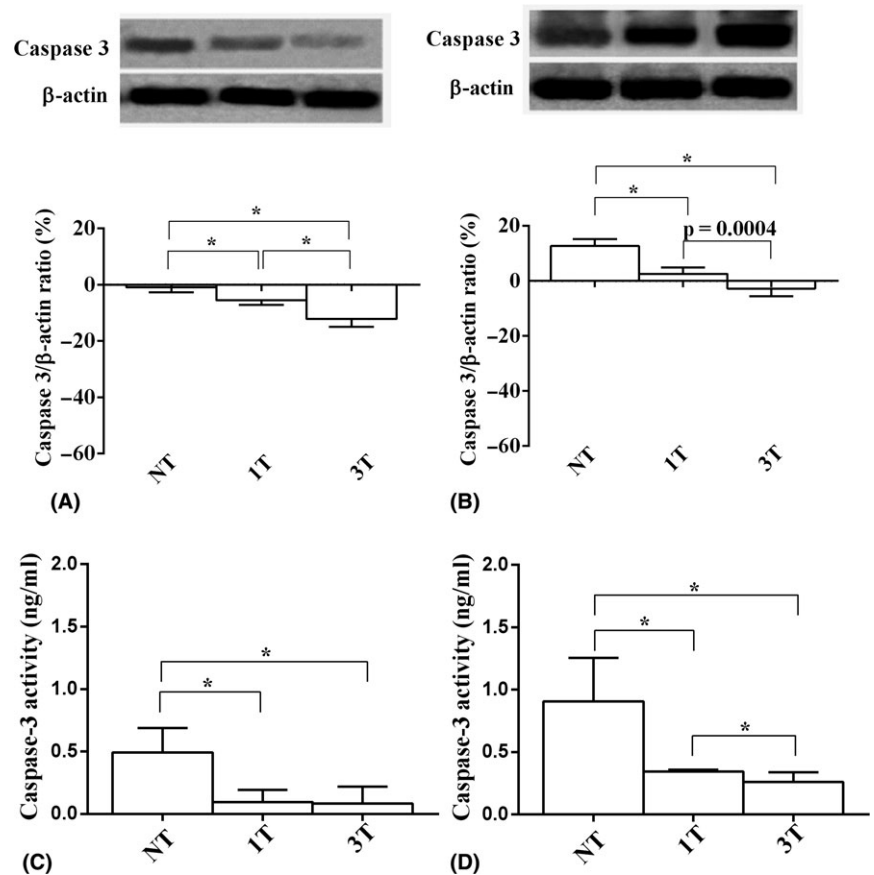


**Fig. 6.** Effects of SMPL on retinal apoptosis in young (A, C) and old (B, D) mice. In (A, B) expression of caspase 3. Densitometric analysis and an example of Western Blot, taken from seven different experiments, are shown. In (C, D) caspase 3 activity is shown. Abbreviations are as in previous Figures. The results are the means ± SD of seven different experiments. Square brackets indicate significance between groups. \*p < 0.0001.

## Results

As shown in Figs 3–9, young and old mice showed different basal values of oxidant/antioxidant system markers; young having higher antioxidants, eNOS and pAkt, while old having higher TBARS, iNOS and apoptosis.

No differences were observed in histological or molecular analysis in the fellow eye between two treatment groups. Thus, only the results found in the right eyes of three-treatment animal group were shown.

SMPL reduced MDA and increased GSH and TrxR1 activity without any histological retinal changes (Figs 3,4).

The antioxidant effects of SMPL were confirmed by Western blot that showed an increase in SOD1 in either the one- or three-treatment group of animals (Fig. 5A,B). Also, the expression of Akt, which would exert protective effects against peroxidation, was found to be augmented by laser treatments (Fig. 5C,D).

In addition, SMPL reduced the markers of apoptosis (Figs 6,7) and increased the autophagic ones (Fig. 8), with particular interest to LC3  $\beta$ .

Finally, both NOS subtypes retinal content were restored by the laser treatment that increased eNOS and reduced iNOS (Fig. 9). It is to note that the total nitrate+nitrite amount was also increased.

As shown by the above Figures, all the effects of SMPL were related to the number of treatments.

## Discussion

The results of this study showed that the SMPL is a treatment option which is able to modulate the oxidant/antioxidant balance within retinal layers, counteract apoptosis and activate autophagy. These findings could be of particular relevance since so far the mechanisms responsible for the protective effects elicited by laser therapy have not yet been clarified.

It is notable that the eyes of young and old mice expressed different amounts of products of lipid peroxidation, expressed by MDA, and of GSH, SOD1 and TrxR1 showing the existence of changes in the balance of oxidant and antioxidant systems as a response to the ageing process. Hence, SOD1 has been reported to be important in protecting the retina from oxidative stress induced

by paraquat and hyperoxia, and by ageing. In addition, SOD1(-/-) mice were found to develop many features of patients with age-related macular degeneration (AMD) (Dong et al. 2009). As has been also reported by Sies et al. (2017), the activation of the selenoprotein TrxR1 could be involved in the regulation of nuclear factor E2-related factor 2 (Nrf2), a peptide belonging to a family of transcription factors inducing antioxidant and detoxication enzymes.

Our study confirmed previous findings about the safety of SMPL. Hence, SMPL is less harmful than continuous wave lasers because, since the pulses are very short, heat can be dissipated within tissue. For the low-intensity/high-density 810 diode laser treatment employed in the current study, prior

clinical studies have shown the absence of retinal damage (Luttrull et al. 2005, 2012; Luttrull & Sinclair 2014; Luttrull 2016a; Luttrull & Margolis 2016b), and improvement of visual function and electrophysiology (Luttrull 2016a, 2018a; Luttrull et al. 2018b). The so-called high-density treatment (by delivering continuous spots on the retina) has been demonstrated to be more effective than the treatment with space among spots, thus with lower number (Lavinsky et al. 2011).

The treatment of left mice eyes with micropulse laser reduced MDA, increased GSH level, SOD1 and TrxR1. Furthermore, those effects, which were evident with the very first treatment in particular in the old eyes, were related to the number of treatments. This issue needs to be further examined to confirm

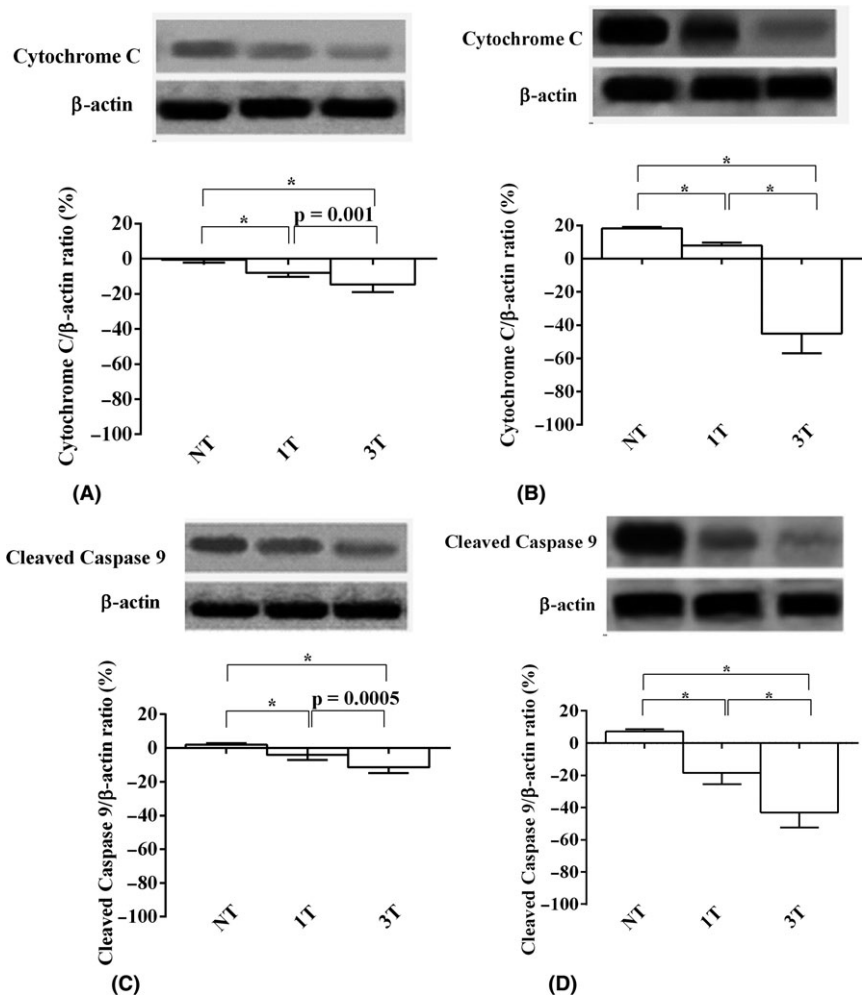


**Fig. 7.** Effects of SMPL on retinal apoptosis in young (A, C) and old (B, D) mice. In (A, B) expression of cytochrome c; in (C, D), expression of cleaved caspase 9. Densitometric analysis and an example of Western Blot, taken from seven different experiments, are shown. Abbreviations are as in previous Figures. The results are the means  $\pm$  SD of seven different experiments. Square brackets indicate significance between groups. \* $p < 0.0001$ .



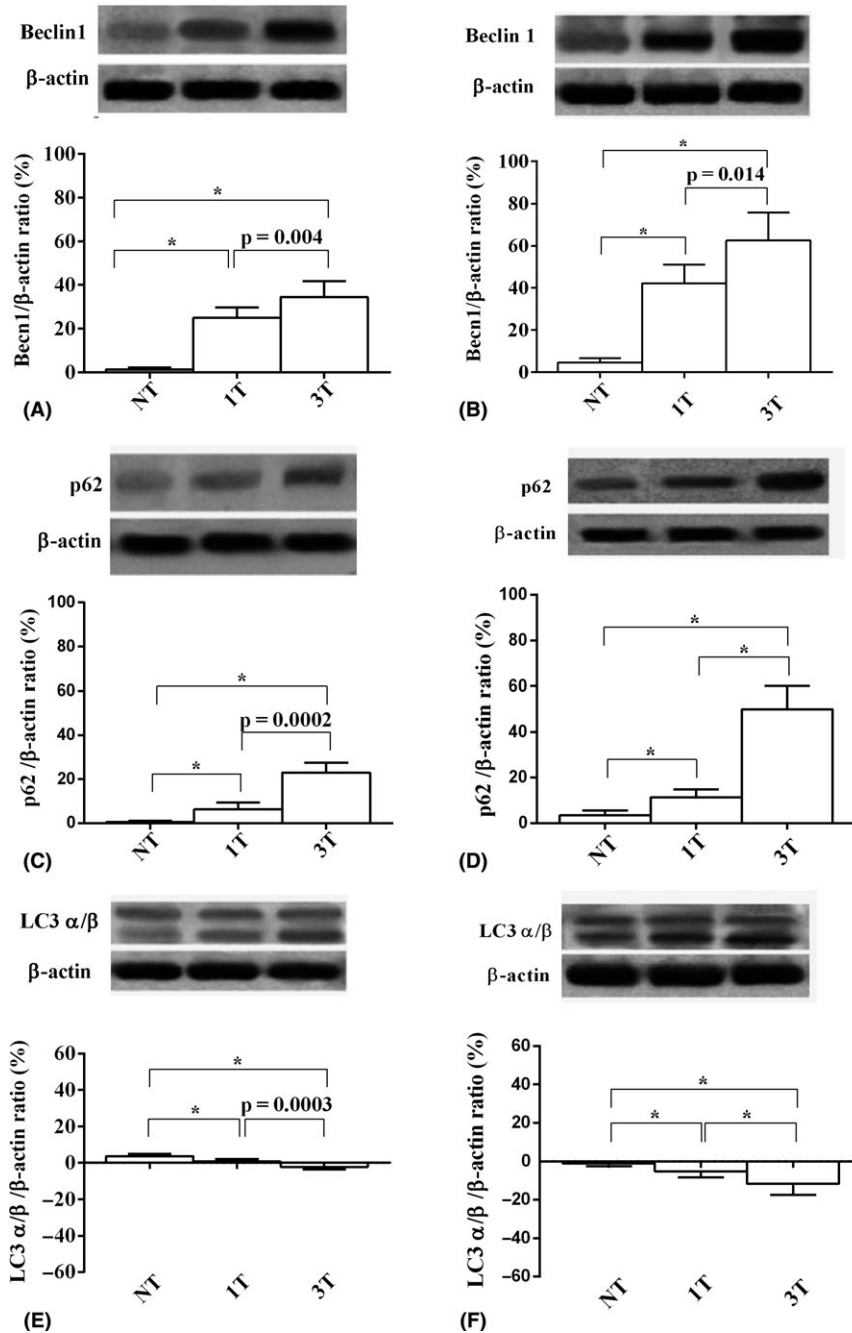


**Fig. 8.** Effects of SMPL on retinal autophagy in young (A, C, E) and old (B, D, F) mice. In (A, B) expression of Beclin 1 (Becn1); in (C, D) expression of p62; in (E, F), expression of LC3 α/β. Densitometric analysis and an example of Western Blot, taken from seven different experiments, are shown. Abbreviations are as in previous Figures. The results are the means ± SD of seven different experiments. Square brackets indicate significance between groups. \**p* < 0.0001.

if this observation is really the result of a cumulative effect caused by SMPL or if it is simply related to a more efficacious wearing off after 1 treatment in comparison with that observed after more treatments. On the ground of current understanding of the main therapeutic pathway via RPE/heat-shock protein (HSP) activation, the proximity effect rather than total dosage could also be

hypothesized to account for our findings.

It is notable that the right eyes were not affected by the micropulse laser irrespective of the number of treatments, which excluded any possible action of laser on the nontreated eye.

In physiological conditions, ROS are normally produced by the RPE of the macula, which has a high metabolic

demand. It is notable, however, that those structures have robust antioxidant systems that protect them from the oxidative stress (Tate et al. 1995; Ruia et al. 2016; Luty 2017).

Any alteration in the oxidant/antioxidant balance may represent the trigger factor at basis of diabetic retinopathy and of macular oedema caused by BRVO (Van der Schaft et al. 1991).

It is interesting to compare our findings with those of prior studies. The stimulation of RPE by a low-dose pulse laser induced hypoxia-inducible factor 1-α (HIF1-α) mRNA and activated an inflammatory response below the acute inflammatory threshold, which could cause tissue injury; in particular, 2 weeks post-treatment, bone marrow-derived cells homing to the RPE-choroid cells were found (Caballero et al. 2017). Moreover, sublethal micropulse photothermal stimulation was shown to upregulate heat-shock protein 70 (Hsp70) in RPE, a protein belonging to the Hsp family members, which functions as molecular chaperones in response to cellular stress like hyper- or hypothermia, hyper- or hypoxia, or oxidative stress (Sramek et al. 2011; Inagaki et al. 2015; Kern et al. 2018).

Since Hsp could counteract the activity of apoptotic and inflammatory pathways that cause cellular damage, upregulation of Hsp70 expression induced by laser irradiation would play an important role in reducing macular oedema following clinical laser therapy. It is notable that the beneficial effects elicited by Hsp70 in the prevention of retinal degenerative disorders could be related to the keeping of cellular redox status by modulation of glutathione-related enzymes.

Thus, although not examined yet, we could hypothesize that the beneficial effects elicited by SMPL are due to changes in HIF1-α and Hsp70 retinal content which might activate forward signalling, possibly accounting for the long-term effects of laser treatment. Those alterations could also be speculated to be involved in the observed differences of responses found between one single treatment and repetitive treatments.

Changes in nitric oxide (NO) release could also play an important role in the pathophysiology of diabetic retinopathy and diabetic macular oedema, by

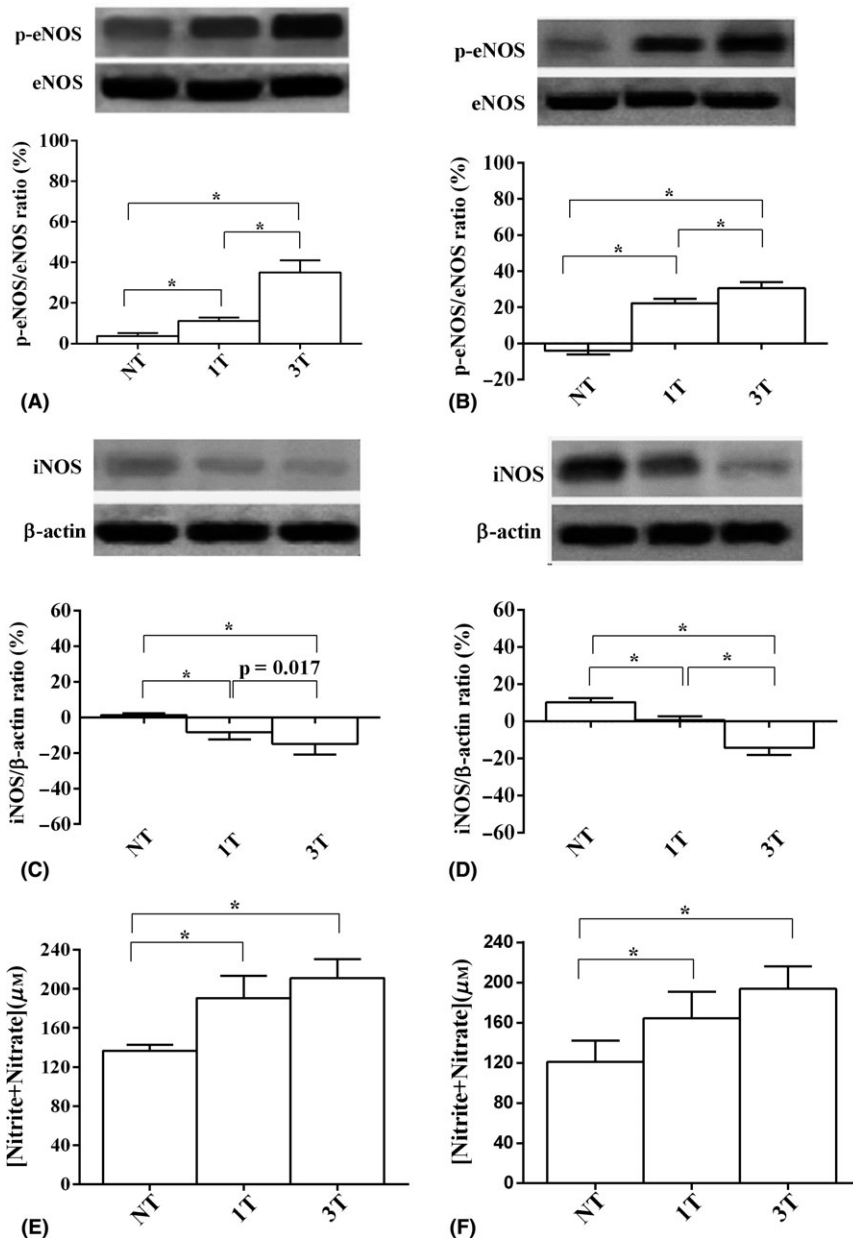


**Fig. 9.** Effects of SMPL on retinal nitric oxide synthase (NOS) content and nitrate and nitrite production in young (A, C, E) and old (B, D, F) mice. In (A, B), endothelial NOS (eNOS) activation; in (C, D) expression of inducible NOS (iNOS). Densitometric analysis and an example of Western Blot, taken from seven different experiments, are shown. In (E, F) nitrite and nitrate retinal content is shown. Abbreviations are as in previous Figures. The results are the means  $\pm$  SD of seven different experiments. Square brackets indicate significance between groups. \* $p < 0.0001$ .

interfering with retinal circulation, the metabolism of photoreceptors and RPE proliferation (Goldstein et al. 1996; Pacher et al. 2005).

NO is synthesized by three different isoforms of NOS: eNOS, neural NOS and iNOS. While NO at low concentration such as that produced by eNOS has been widely reported to maintain good endothelial function, NO produced in large amounts by iNOS has

been regarded as a toxic agent (Awata et al. 2004).

Thus, changes of NO release by NOS/iNOS impairment may represent a pathogenic factor in the acceleration of retinal layers injuries and neovascularization associated with hyperglycaemia, hypertension and ageing (Awata et al. 2004).

In our study, the SMPL treatment restored the levels of eNOS and iNOS,

which were differently expressed in the retina of young and old mice, by increasing the former and decreasing the latter. Our results are in line with recent findings showing that the modulation of angiogenesis by laser treatment could involve the inhibition of iNOS-related NO release by RPE and/or choroid cells (Jiang et al. 2017). Thus, although not fully examined, NOS expressed by those cell types could result from thermal laser effects on the RPE, which is the primary thermal target of SMPL.

In addition, retinal protection exerted by the SMPL could arise, in part, from laser-induced normalization of NOS subtypes' expression. It is noteworthy that nitrates and nitrites content in the retinal tissue was augmented by SMPL. Since the synthesis of nitrate and nitrite could arise from eNOS-related NO release by oxidation reactions, our observations would support the finding of eNOS activation in response to SMPL (Omar et al. 2016).

On the ground of previous findings showing that pan-retinal photocoagulation would inhibit the initiation and maintenance required for active neovascularization through changes of metalloproteinases and their inhibitors balance, further studies would be planned to better address this issue, as well (Flaxel et al. 2007).

Our observations about programmed forms of cell death were in agreement with previous data that showed both an increase in apoptosis and a decrease in the retinal expression of many autophagy markers in old mice (Dunaief et al. 2002). Hence, in our older animals, cytochrome *c*, caspase 9 and caspase 3 expression and activation were higher, whereas Beclin 1, p62 and LC3  $\alpha/\beta$  expression were lower than in young mice.

The role of autophagy in maintaining normal retinal function has been widely demonstrated (Rodríguez-Muela et al. 2013). Moreover, changes in the autophagic pathway were reported to lead to an increased mitochondrial injury and ROS generation (Soufi et al. 2012; Barber & Baccouche 2017; Zhang et al. 2017).

As observed for the oxidant/antioxidant system in our study, apoptosis and autophagy were also modulated by the SMPL treatment, with apoptosis inhibition and autophagy activation. The keeping of a balance between those



programmed forms of cell death could be hypothesized to play a key role in maintaining the physiological retinal function.

Hence, SMPL reduced cytochrome *c*, cleaved caspase 9 and caspase 3 expression and activation, and increased well-known markers of autophagy activation (Wei et al. 2017) like Beclin 1, p62 and LC3 $\beta$ , as shown by the decreased LC3 $\alpha$ / $\beta$  ratio. Thus, the keeping of a balance between those programmed forms of cell death exerted by SMPL could be hypothesized to be involved in normalizing retinal function.

The phosphatidylinositol 3-kinase–Akt (PI3K/AKT) signalling pathway, which is involved in the control of cell survival, differentiation, growth and apoptosis, is activated when retinal layers are exposed to oxidative stress. In particular, it has been found that PI3K/AKT can exert retinal protection against light- or hydrogen peroxide-induced apoptosis by modulation of mitochondrial apoptosis signalling (Zhu et al. 2015). The results of our study would be in agreement with previous observations. Hence, the activated form of Akt was reduced in the old animals in comparison with the young ones. It is notable that as mentioned above, those animals also had higher MDA and lower SOD1, GSH and TrxR1.

Overall, our results lend insight into the physiologic responses to retinal laser treatments sublethal to the retina, such as SMPL, as a clinically safe therapeutic option showing a reduction of oxidative stress, which was accompanied by the modulation of programmed forms of cell death and Akt. Since our findings are in agreement with previous clinical knowledge about this issue (Luttrull 2016a, 2018a; Luttrull et al. 2018b), they could strengthen the use of SMPL as treatment for the management of other retinal disorders characterized by changes in oxidant/antioxidant balance and of apoptosis and autophagy.

## References

- Amoaku WM, Saker S & Stewart EA (2015): A review of therapies for diabetic macular oedema and rationale for combination therapy. *Eye (Lond)* **29**: 1115–1130.
- Awata T, Neda T, Iizuka H et al. (2004): Endothelial nitric oxide synthase gene is associated with diabetic macular edema in type 2 diabetes. *Diabetes Care* **27**: 2184–2190.
- Barber AJ & Baccouche B (2017): Neurodegeneration in diabetic retinopathy: potential for novel therapies. *Vision Res* **139**: 82–92.
- Caballero S, Kent DL, Sengupta N et al. (2017): Bone marrow-derived cell recruitment to the neurosensory retina and retinal pigment epithelial cell layer following subthreshold retinal phototherapy. *Invest Ophthalmol Vis Sci* **58**: 5164–5176.
- De Cillà S, Farruggio S, Vujosevic S et al. (2017): Anti-vascular endothelial growth factors protect retinal pigment epithelium cells against oxidation by modulating nitric oxide release and autophagy. *Cell Physiol Biochem* **42**: 1725–1738.
- Dong A, Xie B, Shen J et al. (2009): Oxidative stress promotes ocular neovascularization. *J Cell Physiol* **219**: 544–552.
- Dunaief JL, Dentchev T, Ying GS & Milam AH (2002): The role of apoptosis in age-related macular degeneration. *Arch Ophthalmol* **120**: 1435–1442.
- Dutta S & Sengupta P (2016): Men and mice: relating their ages. *Life Sci* **152**: 244–248.
- Ferrara N, Gerber HP & LeCouter J (2003): The biology of VEGF and its receptors. *Nat Med* **9**: 669–676.
- Flaxel C, Bradle J, Acott T & Samples JR (2007): Retinal pigment epithelium produces matrix metalloproteinases after laser treatment. *Retina* **27**: 629–634.
- Goldstein I, Ostwald P & Roth S (1996): Nitric oxide: a review of its role in retinal function and disease. *Vision Res* **36**: 2979–2994.
- Grossini E, Pollesello P, Bellofatto K et al. (2014): Protective effects elicited by levosimendan against liver ischemia/reperfusion injury in anesthetized rats. *Liver Transpl* **20**: 361–375.
- Inagaki K, Shuo T, Katakura K et al. (2015): Sublethal photothermal stimulation with a micropulse laser induces heat shock protein expression in ARPE-19 cells. *J Ophthalmol* **2015**: 729–792.
- Jiang H, Wu M, Liu Y et al. (2017): Serine racemase deficiency attenuates choroidal neovascularization and reduces nitric oxide and VEGF levels by retinal pigment epithelial cells. *J Neurochem* **143**: 375–388.
- Kern K, Mertineit CL, Brinkmann R & Miura Y (2018): Expression of heat shock protein 70 and cell death kinetics after different thermal impacts on cultured retinal pigment epithelial cells. *Exp Eye Res* **170**: 117–126.
- Kiire C, Sivaprasad S & Chong V (2011): Subthreshold micropulse laser therapy for retinal disorders. *Retina* **1**: 67–70.
- Lavinsky D, Cardillo JA, Melo LA Jr et al. (2011): Randomized clinical trial evaluating mETDRS versus normal or high-density micropulse photocoagulation for diabetic macular edema. *Invest Ophthalmol Vis Sci* **52**: 4314–4323.
- Li Z, Song Y, Chen X, Chen Z & Ding Q (2015): Biological modulation of mouse RPE cells in response to subthreshold diode micropulse laser treatment. *Cell Biochem Biophys* **73**: 545–552.
- Luttrull JK (2016a): Low-intensity/high-density subthreshold diode micropulse laser (SDM) for central serous chorioretinopathy. *Retina* **36**: 1658–1663.
- Luttrull JK (2018a): Improved retinal and visual function following subthreshold diode micropulse laser (SDM) for retinitis pigmentosa. *Eye (London)* **32**: 1099–1110.
- Luttrull JK & Margolis BW (2016b): Functionally guided retinal protective therapy for dry age-related macular and inherited retinal degenerations: a pilot study. *Invest Ophthalmol Vis Sci* **57**: 265–275.
- Luttrull JK & Sinclair SH (2014): Safety of transfoveal subthreshold diode micropulse laser for fovea-involving diabetic macular edema in eyes with good visual acuity. *Retina* **34**: 2010–2020.
- Luttrull JK, Musch DC & Mainster MA (2005): Subthreshold diode micropulse photocoagulation for the treatment of clinically significant diabetic macular oedema. *Br J Ophthalmol* **89**: 74–80.
- Luttrull JK, Sramek C, Palanker D, Spink CJ & Musch DC (2012): Long-term safety, high-resolution imaging, and tissue temperature modeling of subvisible diode micropulse photocoagulation for retinovascular macular edema. *Retina* **32**: 375–386.
- Luttrull JK, Samples JR, Kent D & Lum BJ (2018b): Pan macular subthreshold diode micropulse laser (SDM) as neuroprotective therapy in primary open-angle glaucoma. In: Samples JR & Paul A (ed.). *Glaucoma Research 2018–2020*. Amsterdam, The Netherlands: Knepper © 2018 Kugler Publications 281–294.
- Lutty GA (2017): Diabetic choroidopathy. *Vision Res* **139**: 161–167.
- Mainster MA (1999): Decreasing retinal photocoagulation damage: principles and techniques. *Semin Ophthalmol* **14**: 200–209.
- Maruko I, Koizumi H, Hasegawa T, Arakawa H & Iida T (2017): Subthreshold 577 nm micropulse laser treatment for central serous chorioretinopathy. *PLoS ONE* **12**: e0184112.
- Ohkoshi K & Yamaguchi T (2010): Subthreshold micropulse diode laser photocoagulation for diabetic macular edema in Japanese patients. *Am J Ophthalmol* **149**: 133–139.
- Omar SA, Webb AJ, Lundberg JO & Weitzberg E (2016): Therapeutic effects of inorganic nitrate and nitrite in cardiovascular and metabolic diseases. *J Intern Med* **279**: 315–336.
- Pacher P, Obrosova I, Mabley J & Szabó C (2005): Role of nitrosative stress and peroxynitrite in the pathogenesis of diabetic complications, emerging new therapeutic strategies. *Curr Med Chem* **12**: 267–275.
- Rodríguez-Muela N, Koga H, García-Ledo L et al. (2013): Balance between autophagic pathways preserves retinal homeostasis. *Aging Cell* **12**: 478–488.

- Ruia S, Saxena S, Prasad S et al. (2016): Correlation of biomarkers thiobarbituric acid reactive substance, nitric oxide and central subfield and cube average thickness in diabetic retinopathy: a cross-sectional study. *Int J Retina Vitreous* **2**: 8.
- Sies H, Berndt C & Jones DP (2017): Oxidative stress. *Annu Rev Biochem* **86**: 715–748.
- Soufi FG, Mohammad-Nejad D & Ahmadi H (2012): Resveratrol improves diabetic retinopathy possibly through oxidative stress - nuclear factor  $\kappa$ B - apoptosis pathway. *Pharmacol Rep* **64**: 1505–1514.
- Sramek C, Mackanos M, Spitler R et al. (2011): Non-damaging retinal phototherapy: dynamic range of heat shock protein expression. *Invest Ophthalmol Vis Sci* **52**: 1780–1787.
- Surico D, Farruggio S, Marotta P et al. (2015): Human chorionic gonadotropin protects vascular endothelial cells from oxidative stress by apoptosis inhibition, cell survival signalling activation and mitochondrial function protection. *Cell Physiol Biochem* **36**: 2108–2120.
- Tate DJ Jr., Miceli MV & Newsome DA (1995): Phagocytosis and H<sub>2</sub>O<sub>2</sub> induce catalase and metallothionein gene expression in human retinal pigment epithelial cells. *Invest Ophthalmol Vis Sci* **36**: 1271–1279.
- Van der Schaft TL, de Bruijn WC, Mooy CM, Ketelaars DA & de Jong PT (1991): Is basal laminar deposit unique for age-related macular degeneration? *Arch Ophthalmol* **109**: 420–425.
- Vujosevic S, Bottega E, Casciano M et al. (2010): Microperimetry and fundus autofluorescence in diabetic macular edema: subthreshold micropulse diode laser versus modified early treatment diabetic retinopathy study laser photocoagulation. *Retina* **30**: 908–916.
- Vujosevic S, Martini F, Convento E et al. (2013): Subthreshold laser therapy for diabetic macular edema: metabolic and safety issues. *Curr Med Chem* **20**: 3267–3271.
- Vujosevic S, Martini F, Longhin E et al. (2015): Subthreshold micropulse yellow laser versus subthreshold micropulse infrared laser in center-involving diabetic macular edema: morphologic and functional safety. *Retina* **35**: 1594–1603.
- Wei H, Xun Z, Granado H, Wu A & Handa JT (2016): An easy, rapid method to isolate RPE cell protein from the mouse eye. *Exp Eye Res* **145**: 450–455.
- Wei J, Ma LS, Liu DJ et al. (2017): Melatonin regulates traumatic optic neuropathy via targeting autophagy. *Eur Rev Med Pharmacol Sci* **21**: 4946–4951.
- Zhang X, Zeng H, Bao S, Wang N & Gillies MC (2014): Diabetic macular edema: new concepts in patho-physiology and treatment. *Cell Biosci* **4**: 27.
- Zhang Y, Cross SD, Stanton JB et al. (2017): Early AMD-like defects in the RPE and retinal degeneration in aged mice with RPE-specific deletion of Atg5 or Atg7. *Mol Vis* **23**: 228–241.
- Zhu C, Wang S, Wang B et al. (2015): 17 $\beta$ -Estradiol up-regulates Nrf2 via PI3K/AKT and estrogen receptor signaling pathways to suppress light-induced degeneration in rat retina. *Neuroscience* **304**: 28–339.

---

Received on May 28th, 2018.  
Accepted on November 16th, 2018.

*Correspondence:*  
Professor Elena Grossini  
Lab. Physiology and Experimental Surgery  
Department of Translational Medicine  
University East Piedmont  
via Solaroli 17, I-28100 Novara  
Italy  
Tel: +390321660526  
Fax: +390321373537  
Email: elena.grossini@med.uniupo.it

We thank Azienda Ospedaliero-Universitaria of Novara for its help.